



ELSEVIER

Thermochimica Acta 248 (1995) 303–318

thermochimica  
acta

## Thermoelectrical analysis of the human skin barrier

W.H.M. Craane-van Hinsberg, J.C. Verhoef, H.E. Junginger,  
H.E. Boddé \*

*Leiden/Amsterdam Center for Drug Research, Division of Pharmaceutical Technology,  
University of Leiden, P.O. Box 9502, 2300 RA Leiden, The Netherlands*

Received 2 January 1994; accepted 2 February 1994

### Abstract

The influence of temperature on the resistive and capacitive properties of human stratum corneum *in vitro* was studied to determine where within substructures of stratum corneum, the electrical resistance  $R$  and capacitance  $C$  components reside. Heating–cooling cycles were designed in accordance with earlier calorimetric and spectroscopic studies of thermal transitions of human stratum corneum lipids and/or proteins. Two different protocols were used. (A) Heat treatment and electrical analysis were carried out simultaneously in pH 7.4 phosphate buffered saline, starting with prehydrated stratum corneum (70% w/w) of pH 7.4. (B) Heat treatment was performed before electrical analysis, using dried stratum corneum (< 10% w/w), followed by prehydration and measurement of the electrical properties in phosphate buffered saline at 20°C. Square-wave alternating current pulses of  $13 \mu\text{A cm}^{-2}$  were applied every 60 s. Analysis of the resulting voltage waveform across stratum corneum yielded an equivalent electrical model of stratum corneum composed of a series connection of two  $RC$  circuits ( $R_1 \parallel C_1$  and  $R_2 \parallel C_2$ ). Below 60°C a constant activation energy of  $5.4 \pm 0.7 \text{ kcal mol}^{-1}$  was measured, which was close to the activation energy of  $\text{K}^+$  diffusion in a fluid aqueous medium. The total resistance of stratum corneum was less than  $100 \text{ k}\Omega \text{ cm}^2$ , which is very low compared to the resistance of black lipid membranes ( $1\text{--}10 \text{ M}\Omega \text{ cm}^2$ ). Both the low activation energy and resistance of human stratum corneum suggest the presence of highly conductive pathways through the membrane. Between 60 and 75°C an abrupt decline of the resistances  $R_1$  and  $R_2$  and a rapid rise of the capacitances  $C_1$  and  $C_2$  was observed. This temperature interval corresponded to the temperature interval of the second thermal transition observed in human stratum corneum, which is a lipid phase transition. Beyond 75°C, the resistances were fairly constant, while the capacitances continued to increase. The changes in the resistances and capacitances brought about by heating to 75 and 95°C were completely irreversible. This is in agreement with X-ray diffraction studies, which

\* Corresponding author.

have shown that the originally predominant lamellar structure with a repeat distance of 6.4 nm does not reappear after recrystallization from 75 and 90°C. The final resistances after heating desiccated stratum corneum ( $\leq 10\%$  w/w hydration) to temperatures of 75 and 95°C and subsequent cooling were less different from the original values than those of hydrated samples, suggesting that the impact of heating depends on the level of stratum corneum hydration. After chloroform–methanol lipid extraction, stratum corneum was characterized by a single *RC* circuit. The resistance of extracted stratum corneum was less than 1% of the original pre-extraction value, which indicates that the resistance of stratum corneum is mainly determined by the intercellular lipids.

Taken together, the correlation between the temperature dependence of the resistances and capacitances between 20 and 75°C suggests that the electrical barrier and the charge storage capacity of stratum corneum are determined by the same substructures. Most probably these structures are the intercellular lipid lamellae, because the changes of the electrical properties mainly take place within the interval 60 to 75°C, which corresponds to the phase transition of free intercellular lipids, and also because these changes are irreversible. This conclusion is also confirmed by chloroform–methanol extraction. However, the continued increases of the capacitances between 75 and 95°C, indicates that the charge storage capacity of stratum corneum also depends on lipids attached to protein. The low resistance and activation energy at temperatures between 20 and 60°C indicate that stratum corneum possesses highly conductive pathways.

*Keywords:* Capacitance; Human skin barrier; Resistance; Skin; TA

---

## 1. Introduction

The relationship between the structure of the skin barrier and its electrical properties is an important field of interest in the development of so called transdermal iontophoretic drug delivery systems, which apply an electrical field across the skin to enhance the transdermal flux of especially charged compounds, for instance peptide or protein drugs [1,2]. Several aspects of iontophoretic transdermal drug delivery, such as skin permeability increase, drug accumulation, flux–voltage dependence, possible side-effects of the system, may be related to electrical properties of the skin.

The electrical resistance of conductance of the skin is a measure of its barrier for ionic transport, while the capacitance of the skin is a measure of its charge storage capacity. These properties have been shown to reside mainly in the stratum corneum, which consists of the most superficial cornified cell layers of the epidermis [3,4]. The electrical properties of the stratum corneum have been modeled as a circuit composed of at least two electrical resistance–capacitance (*RC*) circuits connected in series [5,6].

Electron microscopic and histological studies have revealed many details about the complex structure of stratum corneum. This tissue consists of 20–30 layers of flattened epidermal cells, which contain densely packed bundles of keratin filaments embedded in a keratohyalin matrix [7]. Each such cell is surrounded by a so called

corneocyte envelope, which consists of protein (involucrin) on the outside of which there is a layer of  $\omega$ -hydroxyceramides, most probably linked to it by ester bonds [8]. In the remaining space between corneocytes we find multiple sheets of lipids, composed mainly of ceramides, cholesterol, fatty acids and triglycerides [9]. The intercellular lipid lamellae are arranged according to the so called Landmann unit [10], composed of two (broad) bilayers and one (narrow) monolayer according to the sequence broad–narrow–broad. Junctions between opposing corneocytes are formed by protein aggregates, called desmosomes. The corneocytes gradually dehydrate and the intercellular cohesion disintegrates as corneocytes migrate to the skin surface, resulting ultimately in desquamation of superficial cells [11].

Although the structure of stratum corneum is basically known, the connection between its structural and its electrical components ( $R_1||C_1$  and  $R_2||C_2$ ) is still unclear. In an effort to understand this relationship an approach based on differential thermal analysis was followed. Between 20 and 120°C four thermal transitions take place within human stratum corneum, namely at 40, 70, 85 and 107°C [12]. These thermal transitions have been studied closely by X-ray diffraction and Fourier transform infrared spectroscopy and could be attributed to phase transitions of either free lipids, protein-bound lipids or proteins [13–15]. In the present study, the electrical resistances and capacitances of stratum corneum were measured while stratum corneum was heated to one of four selected maximum temperatures and subsequently cooled. The maximum temperature of each heating–cooling cycle was chosen between two sequential thermal transitions, which allowed possible effects to be related to a particular phase transition.

## 2. Experimental section

### 2.1. Isolation of stratum corneum

The present study was performed with human abdominal skin obtained from a single donor. It was used within 24 h after cosmetic surgery. The subcutaneous fat was removed and the stratum corneum surface cleaned with a moist tissue. Skin was dermatomed at a thickness of about 300  $\mu\text{m}$  and spread, dermal side down, on a Whatman paper soaked in a 0.2% trypsin (type III; from bovine pancreas; Sigma Chemicals, The Netherlands) solution in 0.15 M phosphate buffered saline (PBS) of pH 7.4. The skin was incubated overnight with the enzyme solution at 4°C and then for 1 h at 37°C. After the enzyme treatment the stratum corneum layer was only loosely connected to the underlying epidermis cells and was carefully separated using a pair of tweezers. Remaining trypsin activity was blocked by submerging the stratum corneum in a 0.2% solution of trypsin inhibitor (type II-S from soybean; Sigma Chemicals, The Netherlands). The stratum corneum was washed twice in twice-distilled water and subsequently dried and stored in a desiccator over silica gel. The desiccator was filled with nitrogen gas to inhibit oxidation of lipids and proteins.

## 2.2. Chloroform–methanol extraction

Lipid extraction was performed by bathing stratum corneum overnight in a 2:1 (v/v) mixture of chloroform and methanol at 4°C in a shaker bath. The stratum corneum was removed from the chloroform–methanol mixture, prehydrated and mounted in the transport cells for measurement of the electrical properties. Directly after lipid extraction stratum corneum was prepared for electron microscopy.

## 2.3. Electron microscopic visualisation of lipid-extracted stratum corneum

The stratum corneum samples were cut in small pieces ( $1 \times 3 \text{ mm}^2$ ) and fixed for 2 h in 2% glutaraldehyde in 0.1 M cacodylate buffer at pH 7.4 and 4°C. After rinsing twice for 30 min with cacodylate buffer, the tissue was post-fixed for 1 h in 2% osmium tetroxide in veronal buffer at pH 7.4 and 4°C. Then the tissue was washed twice for 30 min in veronal buffer. Removal of water from the fixed tissue was performed by transferring the tissue through a graded series of ethanol–water solutions, from 30 to 100% ethanol. A 15–30 min equilibration was allowed in each solution. Subsequently, the tissue was impregnated with propylene oxide at room temperature, then infiltrated with a solution of 50% propylene oxide in Epon 812 for 2 h and finally with pure Epon 812 for 16 h. The stratum corneum samples were orientated flatly and horizontally in the supporting material. The epoxy resin Epon was allowed to polymerize and harden at a temperature of 35°C for 16 h, then heated to 60°C for 48 h. From the tissue blocks ultra-thin 80 nm sections were cut using a microtome and these were examined under a Philips 410 transmission electron microscope.

## 2.4. Stratum corneum hydration

To hydrate stratum corneum, it was punched into disks of 16 mm diameter, which were then placed on a plastic grid above 0.15 M PBS for 48 h at 4°C. Then the disks were submerged in 0.15 M PBS and allowed to equilibrate to the buffer for 2 h. The weight of stratum corneum was measured before and after hydration and the difference between wet weight  $g_w$  and dry weight  $g_d$  calculated for each stratum corneum sample. The hydration level was expressed as the difference between wet and dry weight, divided by the wet weight:  $(g_w - g_d)/g_w$ . After hydration the hydration level was  $0.72 \pm 0.05 \text{ g/g}$ . The hydrated stratum corneum samples were mounted in two-compartment transport cells, which were filled with 0.15 M PBS at pH 7.4.

## 2.5. Transport cell

The perspex transport cells consisted of two compartments, between which a piece of hydrated stratum corneum was clamped, leaving a  $0.79 \text{ cm}^2$  surface area for transport (Fig. 1). Both compartments were filled with the same 0.15 M PBS at pH 7.4 and connected to a circulating system for two purposes: (a) to provide a means

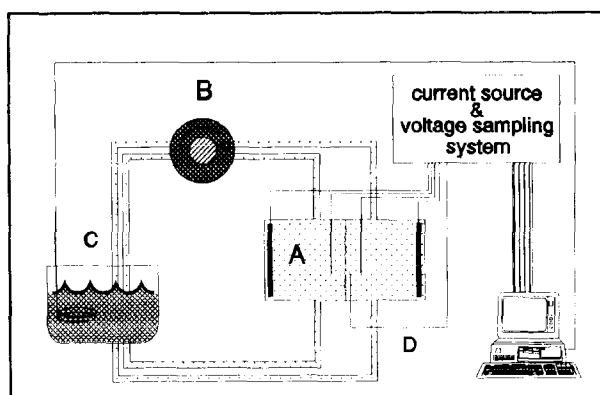


Fig. 1. Experimental setup for temperature and electrical current treatment of human stratum corneum in vitro. The stratum corneum is mounted between the two compartments of the transport cell A, each compartment of which contains a current delivery Ag/AgCl plate electrode and a voltage measuring Ag/AgCl bar electrode; the voltage measuring electrodes are placed 1 mm from the skin surface and the electrodes are connected to a computer controlled current source and voltage sample device. B is the circulating system, C is the programmable waterbath and D is the Ni/CrNi thermocouple.

for external stirring of the buffer and hence avoid stagnant layers, and (b) to control the skin temperature.

### 2.6. Buffer

Twice-distilled water was used for the preparation of isotonic PBS. The buffer was composed of 0.149 M NaCl, 2 mM  $\text{KH}_2\text{PO}_4$  and 2 mM  $\text{NaHPO}_4$ , and adjusted to pH 7.4 with phosphoric acid.

### 2.7. Skin temperature control

The buffer solutions were circulated between thermally controlled reservoirs and each of the cell compartments (Fig. 1). The reservoirs were placed in a programmable waterbath (type SW1, Julabo Labortechnik GMBH, Seelbach, Germany). The temperature inside the transport cells, near the skin surfaces, was monitored by a Ni/Cr–Ni thermosensor (Shimaden Sr35-3111, Japan), placed 0.5 mm from the skin surfaces. The heating–cooling programme of the waterbath was such that the rate of temperature change inside the diffusion cells was  $2.5 \text{ K min}^{-1}$ .

Samples of prehydrated stratum corneum were subjected to three different heating–cooling cycles during which the impedance of stratum corneum was measured at regular intervals: (1) from 20 to 45°C and back; (2) from 20 to 80°C and back; and (3) from 20 to 95°C and back. The maximally attainable temperature of stratum corneum inside the transport cells without disturbance of the electrical measurements by boiling of the buffer was 95°C.

In a second series of experiments, desiccated stratum corneum samples were wrapped in aluminum foil and incubated in a stove at 45, 80, 90 or 120°C for 10 min. Then the samples were cooled to room temperature, hydrated and mounted into the iontophoresis cells, whereafter the resistance and capacitance values were measured.

### 2.8. Voltage waveform analysis

Each compartment of the transport cell contained a Ag/AgCl current delivering plate electrode and a Ag/AgCl voltage measuring bar electrode. The current source was programmed to deliver a train of alternating current pulses for 1 s each minute, starting with a positive 10  $\mu\text{A}$  amplitude (13  $\mu\text{A cm}^{-2}$  current density) for 5 ms, after which the current was switched off for 5 ms, followed by a negative 10  $\mu\text{A}$  amplitude (13  $\mu\text{A cm}^{-2}$  current density) for 5 ms and completed with a 5 ms current-off period.

The voltage measuring electrodes were positioned at a distance of 2 mm from the tissue surface (Fig. 1). The voltage wave was sampled at regular intervals using a 10 MHz sampling unit. The voltage data were stored in the computer and analyzed by means of an exponential least squares fit programme, based on the Levi–Marquardt algorithm.

Throughout this paper, resistances and capacitances are given as the mean  $\pm$  S.D. of  $n \geq 6$  samples.

### 2.9. Calculation of activation energies

The activation energy  $E_a$  for the passage of ions through the skin barrier was calculated from the slope of an Arrhenius plot of the natural logarithm of the conductance  $\ln G$  versus the reciprocal of the absolute temperature  $1/T$ , and analyzing the data according to an Arrhenius relationship

$$\ln G = A - E_a/RT \quad (1)$$

in which  $A$  represents a pre-exponential factor and  $R$  is the universal gas constant. Activation energies are presented as the mean  $\pm$  S.D. of  $n \geq 6$  experiments.

## 3. Results

Control experiments in which the temperature was maintained at 20°C for 2 h, revealed that the resistances and capacitances remained constant (Table 1). These observations indicated that the small 13  $\mu\text{A cm}^{-2}$  current itself did not affect the conductance and capacitance properties of stratum corneum.

Now consider the temperature dependent changes observed in the resistances and capacitances of the stratum corneum presented in Fig. 2 and Table 2. For clarity, three temperature intervals will be discussed separately: a lower (20–60°C), a middle (60–75°C) and a higher (75–95°C) temperature interval.

Table 1  
Effect of time on the resistances and capacitances of human stratum corneum submerged in 0.15 M phosphate buffered saline at a constant temperature of 20°C<sup>a</sup>

Time/h	$R_1/$ k $\Omega$ cm <sup>2</sup>	$R_2/$ k $\Omega$ cm <sup>2</sup>	$C_1/$ 10 <sup>-9</sup> Farad cm <sup>-2</sup>	$C_2/$ 10 <sup>-8</sup> Farad cm <sup>-2</sup>
0	30.0 ± 6.3	37.7 ± 7.2	2.1 ± 0.7	1.4 ± 0.5
2	26.9 ± 2.0	32.5 ± 6.1	2.5 ± 0.6	1.7 ± 0.6

<sup>a</sup> Data represent the mean ± S.D. of  $n \geq 6$  samples.

Table 2  
Effect of temperature on the resistances and capacitances of human stratum corneum<sup>a</sup>

$t/$ °C	$R_1/$ k $\Omega$ cm <sup>2</sup>	$R_2/$ k $\Omega$ cm <sup>2</sup>	$C_1/$ 10 <sup>-9</sup> Farad cm <sup>-2</sup>	$C_2/$ 10 <sup>-8</sup> Farad cm <sup>-2</sup>
20	20.5 ± 5.4	46.0 ± 25.2	2.4 ± 0.8	1.9 ± 1.3
60	11.3 ± 2.0	29.2 ± 19.6	1.5 ± 0.7	3.3 ± 1.5
75	0.5 ± 0.1	0.8 ± 0.7	13.6 ± 10.3	26.6 ± 21.3
95	0.3 ± 0.2	0.2 ± 0.1	3.7 ± 1.4	104.0 ± 50.8

<sup>a</sup> Data represent the mean ± S.D. of  $n \geq 6$  samples.

### 3.1. Lower temperature interval (20–60°C)

During an increase of temperature from 20 to 60°C, the resistances  $R_1$  and  $R_2$  decreased gradually to 55% and 63%, respectively, of their initial values. Meanwhile the capacitances remained fairly constant (Fig. 2(A) and (B), Table 2). The Arrhenius plot corresponding to the temperature interval between 20 and 60°C was linear. The slope of the Arrhenius plot yielded an activation energy of  $5.4 \pm 0.7$  kcal mol<sup>-1</sup> (Fig. 3).

### 3.2. Middle temperature interval (60–75°C)

When temperatures exceeded 60°C, an abrupt fall of the resistances and a sudden increase of the capacitances were observed. At 75°C, the total resistance had decreased by two orders of magnitude and came close to the resistance of the buffer (Fig. 2(A) and (B); Table 2). In fact, an abrupt thermal transition of both electrical properties took place within the middle temperature interval.

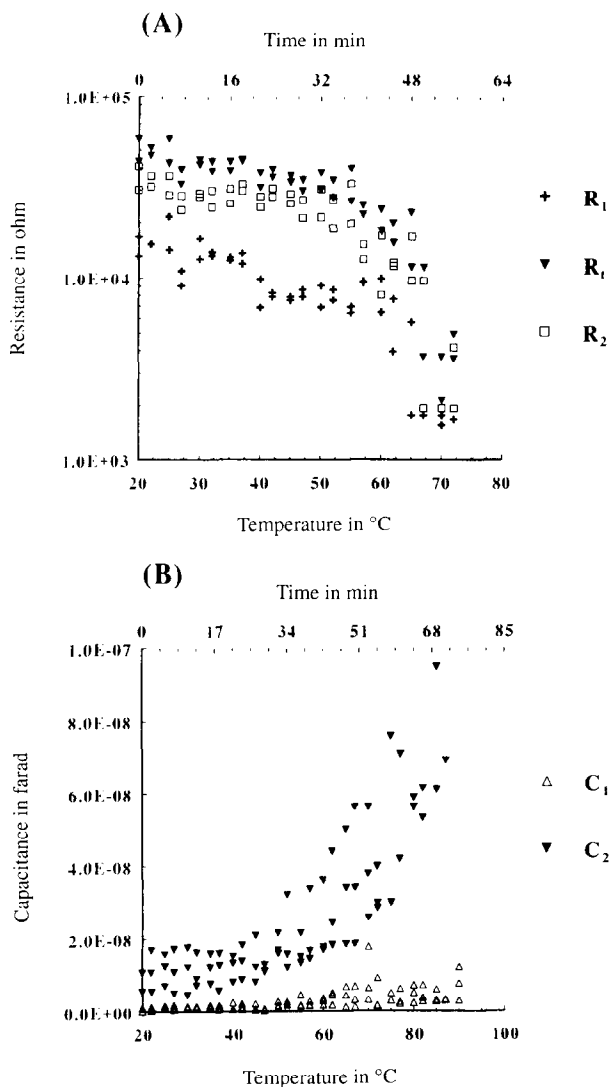


Fig. 2. Temperature dependence of the resistances and capacitances of human stratum corneum. (A) Total resistance  $R_t$  and resistance components  $R_1$  and  $R_2$  are plotted against temperature. (B) Capacitance components,  $C_1$  and  $C_2$ , are plotted as a function of temperature.

### 3.3. Higher temperature interval (75–95°C)

Between 75 and 95°C no significant decrease of the resistances was observed. The capacitances continued to increase from 75 to 95°C (Table 2). Beyond 75°C, the Arrhenius plot was found to be almost horizontal (Fig. 3).



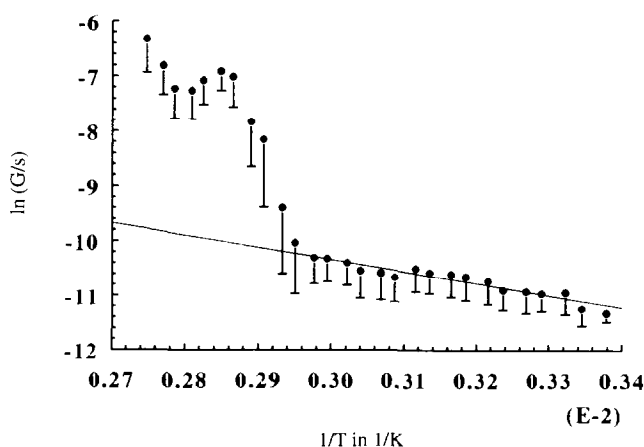


Fig. 3. Arrhenius plot of the electrical conductance of human stratum corneum in vitro. The natural logarithm of the electrical conductance  $\ln G$  is plotted versus the inverse of the absolute temperature  $1/T$ . The data represent mean  $\pm$  standard deviation of  $n = 6$  samples. The slope of the linear part of the plot corresponding to the temperature interval 20–60°C is  $5.4 \pm 0.7$  kcal mol<sup>-1</sup> ( $R^2 = 0.92$ ).

### 3.4. Reversibility

The increase of the capacitances and resistances was reversible when the maximum temperature was 45°C, but irreversible when the maximum temperature was 75°C or higher. When desiccated instead of 70% hydrated stratum corneum was subjected to maximum temperatures of 45 or 75°C and subsequently cooled, the same resistance and capacitance values were measured as before heating. When desiccated stratum corneum was exposed to temperatures of 95 and 120°C and subsequently cooled, the final capacitance  $C_1$  was significantly smaller, though the final capacitance  $C_2$  was about 10 times higher than their original values at 20°C (Figs. 4(A), (B), 5(A), (B)).

### 3.5. Chloroform–methanol extraction

Electron micrographs of normal stratum corneum show intercellular spaces filled with gray material, which represent the intercellular lipids (Fig. 6(A)). The intercellular spaces of chloroform–methanol extracted stratum corneum were completely transparent, indicating that the intercellular lipids were extracted from the samples (Fig. 6(B)). Table 3 shows the resistance and capacitance data of not-extracted, chloroform–methanol extracted stratum corneum samples and of pure buffer. Before chloroform–methanol extraction, the electrical properties of stratum corneum were characterized by two resistances and capacitances. After extraction only one resistance was measured, which was about 0.8% of the total original resistance and which was almost equal to the resistance of pure buffer. Besides a resistance, lipid-extracted stratum corneum also possessed one capacitance, with a value close to the original  $C_1$  (Table 3).

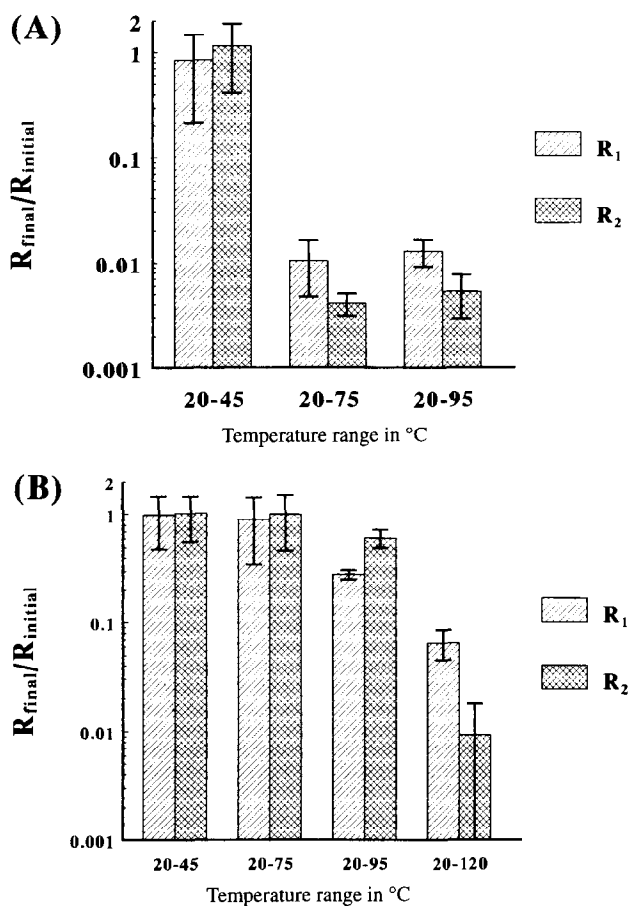


Fig. 4. Ratio between final and initial values of the resistances  $R_1$  and  $R_2$ . The resistance was measured at 20°C. Human stratum corneum samples were heated to a maximum temperature of 45, 75, 95 or 120°C and then cooled to 20°C, after which the final resistance was measured. (A) Hydrated stratum corneum. (B) Dried stratum corneum. The data represent the mean  $\pm$  S.D. of six stratum corneum samples.

#### 4. Discussion

In the experiments presented in this study, a low resistance contact between the voltage measuring electrodes and the stratum corneum sample was maintained by a 0.15 M PBS solution. The ionic content comprised 97% NaCl and 3% phosphoric acid, which was added to provide a constant pH of 7.4. The reason for buffering the medium was that the permeability of stratum corneum is influenced by the pH of the medium. Studies on electrical transport of endogenous ions in stratum corneum have shown that transport rates are determined by the pH of the surrounding medium [16].

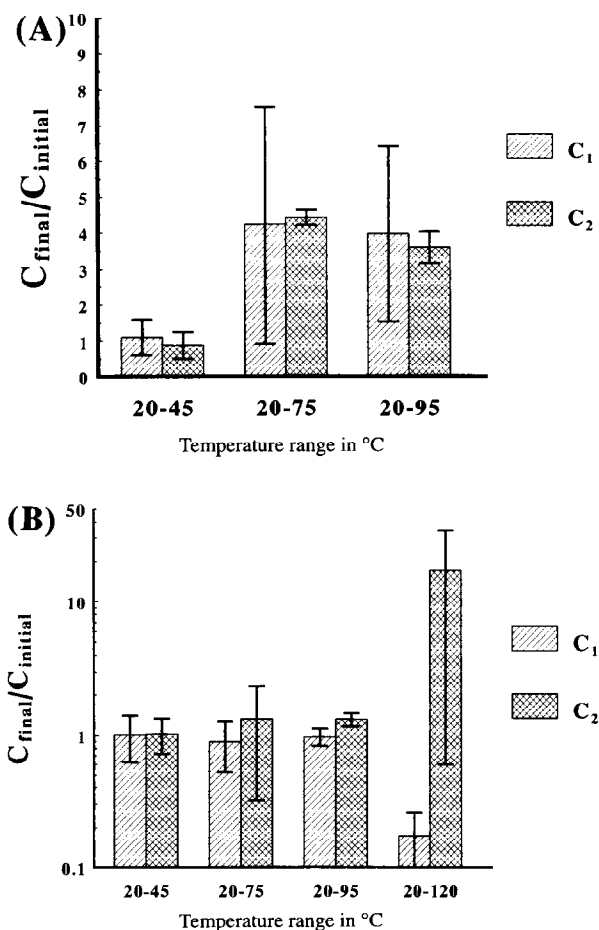


Fig. 5. Ratio between final and initial values of the human stratum corneum capacitances  $C_1$  and  $C_2$ . The initial capacitances were measured at 20°C. Then stratum corneum samples were heated to a maximum temperature of 45, 80, 95 or 120°C and then cooled to 20°C, after which the final values of the capacitances were measured. (A) Hydrated stratum corneum. (B) Dried stratum corneum. The data represent the mean  $\pm$  S.D. of six stratum corneum samples.

The transport number, defined as the fraction of the total current carried by a particular ion, has been calculated for  $\text{Na}^+$  and  $\text{Cl}^-$  in human stratum corneum in vitro at pH 7.4 at 21°C and 37°C for NaCl concentrations of 0.15 M. At both measured temperatures, the transport numbers are 60% for  $\text{Na}^+$  and 40% for  $\text{Cl}^-$ , respectively, indicating that the ionic current through human stratum corneum is carried primarily by  $\text{Na}^+$  and  $\text{Cl}^-$  [17]. Therefore, it is most likely in the present study that the electrical conductance or resistance and the activation energy are mainly determined by the electrical transport of  $\text{Na}^+$  and  $\text{Cl}^-$  through human stratum corneum.

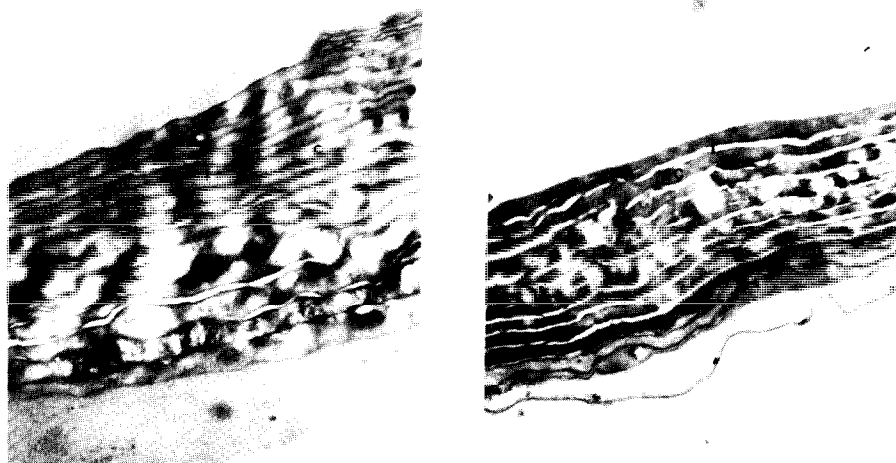


Fig. 6. Effects of methanol-chloroform extraction on the ultrastructure of stratum corneum. (A) Control stratum corneum sample; original magnification  $\times 10\,500$ . (B) Methanol-chloroform extracted stratum corneum; original magnification  $\times 10\,500$ . c, Corneocytes; i, intercellular space.

Table 3  
Resistance and capacitance before and after lipid extraction<sup>a</sup>

Extracted	$R_1/$ $\text{k}\Omega\text{ cm}^2$	$R_2/$ $\text{k}\Omega\text{ cm}^2$	$C_1/$ $10^{-9}\text{ Farad cm}^{-2}$	$C_2/$ $10^{-8}\text{ Farad cm}^{-2}$
–	33.2 $\pm 6.2$	40.1 $\pm 2.3$	1.3 $\pm 0.4$	3.0 $\pm 0.4$
+	0.6 $\pm 0.1$	–	1.9 $\pm 0.3$	–
Buffer only	0.07 $\pm 0.05$	–	0.013 $\pm 0.004$	–

<sup>a</sup> Data represent the mean  $\pm$  S.D. of  $n \geq 6$  samples.

The mean current density during the experiments was zero, but at 1 min intervals the current density was  $+13\ \mu\text{A cm}^{-2}$  for 5 ms and  $-13\ \mu\text{A cm}^{-2}$  for 5 ms. The resistances of stratum corneum which was kept at  $20^\circ\text{C}$  remained unchanged, indicating the momentary  $13\ \mu\text{A cm}^{-2}$  current density did not by itself induce changes of the electrical resistance. This result is in agreement with studies on the current density dependence of human skin resistance, which have shown that only current densities higher than  $15\ \mu\text{A cm}^{-2}$  alter the resistance of human skin [18].

#### 4.1. Lower temperature interval (20–60°C)

The resistances decreased and the capacitances increased gradually from 20 to  $60^\circ\text{C}$  without showing any abrupt change around  $40^\circ\text{C}$ , which suggests that the

thermal transition at 40°C has no influence on the electrical properties of stratum corneum. The thermal transition at 40°C has been studied by X-ray diffraction and has been ascribed to a lateral phase transition of the intercellular non-protein bound lipids, which are ordered in lamellar layers [15]. Below 40°C the lateral arrangement of these lipids within a lamellar layer is predominantly orthorhombic. During the first thermal transition with midpoint around 40°C the lateral arrangement changes from orthorhombic to hexagonal.

Between 20 and 60°C the Arrhenius plot was straight ( $R^2$  0.903), indicating that the electrical barrier for sodium and chloride transport within this temperature interval was characterized by a single activation energy. The linearity of the Arrhenius plot in the 20–60°C interval is in agreement with the reversibility of the stratum corneum barrier in that interval (see Section 4.4) and warrants calculation of an activation energy.

The fact that stratum corneum had a relatively low electrical resistance ( $\pm 100$  k $\Omega$  cm<sup>2</sup>) compared to black lipid films (1–10 M $\Omega$  cm<sup>2</sup>) strongly suggests the presence of highly conductive pathways [19]. The presence of highly conductive pathways is furthermore suggested by the value found for the activation energy for ionic current through stratum corneum. In this study an activation energy of  $5.4 \pm 0.7$  kcal mol<sup>-1</sup> was calculated, which is close to the activation energy of  $6.9 \pm 1.2$  kcal mol<sup>-1</sup> determined for the diffusion of K<sup>+</sup> in a fluid aqueous environment [20].

#### 4.2. Middle temperature interval (60–75°C)

Between 60 and 75°C the resistances decreased abruptly. The decrease of resistance was accompanied by an increase of the capacitances. The resistance decrease and capacitance increase mainly took place within this temperature interval. Around 75°C the total stratum corneum resistance came close to the resistance of pure phosphate buffer. Interestingly, this thermal transition of the electrical resistances and capacitances corresponds well with the second thermal transition, observed in differential thermal analysis studies of human stratum corneum, which has been attributed to lipids not attached to protein. Further investigation of this thermal transition by X-ray diffraction has shown that this transition is caused by a disordering of the intercellular lamellar lipid phase [13–15].

At 60°C an abrupt change in the slope of the Arrhenius plot was observed, marking the onset of changes in the barrier properties of stratum corneum. The calculation of an activation energy between 60 and 75°C is meaningless, because the stratum corneum was subject to structural changes within this temperature interval.

#### 4.3. Higher temperature interval (75–95°C)

The capacitances continued to increase from 75 to 95°C, indicating that their magnitude also depends on protein-bound lipids, which undergo a thermal transition at around 85°C [13]. Beyond 75°C no significant decrease of the resistances was observed and the slope of the Arrhenius plot between 75 and 95°C was almost zero, indicating an almost complete breakdown of the electrical barrier.

#### 4.4. Reversibility

The resistances and capacitances recovered completely after stratum corneum was heated to 45°C and subsequently cooled. However, the thermal transitions of the resistances and capacitances no longer returned to their original values after stratum corneum was allowed to cool from temperatures of 75°C and 95°C. Apparently, the thermal transitions of the resistances and capacitances between 70 and 85°C are irreversible. This also corresponds to observations made by X-ray diffraction, which have shown that upon cooling from temperatures of 75 and 90°C the originally predominant repeat distance of 6.4 nm did not reappear, but the lipids preferentially recrystallized in one lamellar structure with a repeat distance of 13.4 nm [13], which was only present in small amounts before heating.

Effects of heating on the conductance and the capacitances appeared to be less reversible or more profound at 70% stratum corneum hydration than at 10%, suggesting that the degree of hydration determines the impact of heating on the structure of stratum corneum. Also in X-ray diffraction studies an influence of hydration on the bilayer structure has been observed; the X-ray scattering curves of stratum corneum samples hydrated to 40% or higher showed a reflection at 13.4 nm repeat distance, which was less intense than at lower hydration levels, indicating a decrease in longitudinal lipid lamellar order with increasing hydration [13].

#### 4.5. Chloroform–methanol extraction

The electron micrographs of chloroform-extracted stratum corneum, which were prepared using conventional osmium tetroxide fixation procedures, show that the intercellular lipids are no longer present. Lipid analysis and electron microscopic studies using ruthenium fixation have shown that the free intercellular lipids, but not the protein-bound lipids are removed by chloroform–methanol extraction [21–23]. The enormous increase in the conductance of stratum corneum caused by the extraction can therefore be attributed to the removal of the intercellular lipid lamellar phase, indicating also that these lipids mainly determine the magnitude of the electrical barrier. The single capacitance left after lipid extraction suggests that one of the original capacitances has been removed by the extraction procedure and therefore mainly depends on free intercellular lipids, while the other capacitance, which is left after lipid extraction, largely depends on protein-bound lipids.

### 5. Conclusions

The temperature dependence of the capacitances and conductances have much in common, (1) a gradual reversible increase at low temperatures, and (2) a rapid increase between 60 and 75°C. This indicates that the capacitances and conductances of stratum corneum are mutually related and probably determined by the same substructures of stratum corneum.

The main electrical barrier and the charge storage capacity both appear to reside within the intercellular lipid lamellae. This conclusion is supported by three observations made in this study:

(1) A sudden decrease of the resistances and increase of the capacitances occurs within the temperature interval corresponding to the phase transition of the intercellular lipids.

(2) The thermal transitions of the electrical resistances and capacitances observed between 60 and 75°C are completely irreversible.

(3) Chloroform–methanol extraction of the intercellular lipids completely annihilates the stratum corneum electrical resistance and leaves only one capacitance.

The increase of both the capacitances is continued between 75 and 95°C, showing that their values also depend on protein-bound lipids. A connection between protein-bound lipids and at least one of the capacitances of stratum corneum was confirmed by the effect of chloroform extraction on the charge storage properties of stratum corneum.

The low resistance compared to black lipid films and the low activation energy in the low temperature range, which is close to the activation of ion diffusion in an aqueous medium indicate the presence of highly conductive pathways.

## Appendix

Electrically, stratum corneum behaves as a low-pass filter; the voltage resulting from an applied pulsed current  $I$  follows an exponential rise and decay. A previously reported study showed that a bi-exponential equation gave a more adequate fit of the voltage time course than a single exponential fit, suggesting that the equivalent electrical circuit of stratum corneum consisted of at least two parallel resistance–capacitance elements ordered in series [3]. The voltage decay  $V(t)$  can be mathematically expressed by Eq. (A1), in which  $\tau_1$  and  $\tau_2$  are the two time constants determining the decay rate and  $V_\infty$  is a residual voltage (Eq. (A2)). The capacitance ( $C_1$  and  $C_2$ ) and resistance components ( $R_1$  and  $R_2$ ) are calculated according to Eqs. (A3) and (A4) respectively.

$$V(t) = V_1 e^{-t/\tau_1} + V_2 e^{-t/\tau_2} + V_\infty \quad (\text{A1})$$

$$V_\infty = \lim_{t \rightarrow \infty} V(t) \quad (\text{A2})$$

$$R_1 = \frac{V_1}{I} \quad R_2 = \frac{V_2}{I} \quad (\text{A3})$$

$$C_1 = \frac{\tau_1}{R_1} \quad C_2 = \frac{\tau_2}{R_2} \quad (\text{A4})$$

## References

- [1] P.G. Green, M. Flanagan, B. Shroet and R.H. Guy, Iontophoretic drug delivery, *Pharmaceutical Skin Penetration Enhancers*, 59 (1993) 311–334.

- [2] S. Singh and J. Singh, Transdermal drug delivery by passive diffusion and iontophoresis: A review. *Med. Res. Rev.*, 13(5) (1993) 569–621.
- [3] T. Rosendal, Studies on the conducting properties of human skin to direct current. *Acta Physiol. Scand.*, 5 (1943) 130–151.
- [4] J.C. Lawler, M.J. Davis and E.C. Griffith, The electrical impedance of the surface sheath of skin and deep tissues. *J. Invest. Dermatol.*, 34 (1960) 301–308.
- [5] D.T. Lykken, Square-wave analysis of skin impedance. *Psychophysiology*, 7 (1971) 262–275.
- [6] R.T. Tregear, *Physical Functions of Skin*, Academic Press, London, 1966, pp. 53–72.
- [7] R.J. Scheuplein and I.H. Blank, Permeability of the skin, *Physiol. Rev.*, 51 (1991) 702–747.
- [8] D.T. Downing, Lipid and protein structures in the permeability barrier of mammalian epidermis. *J. Lipid Res.*, 33 (1992) 301–313.
- [9] P.W. Wertz, P.S. Cox, C.A. Squier and D.T. Downing, Lipids of epidermis and keratinized and nonkeratinized oral epithelia, *Comp. Biochem. Physiol. B*, 83 (1985) 229–232.
- [10] L. Landmann, The epidermal permeability barrier. *Anat. Embryol.*, 178 (1988) 1–13.
- [11] P.M. Elias, Epidermal lipids, barrier function, and desquamation, *J. Invest. Dermatol.*, 80 (1983) 44–49.
- [12] J.A. Bouwstra, M.A. De Vries, G.S. Gooris, W. Bras, J. Brussee and M. Ponc, Thermodynamic and structural aspects of the skin barrier, *J. Controlled Release*, 16 (1991) 209–220.
- [13] J.A. Bouwstra, G.S. Gooris, J.A. van der Spek and W. Bras, The structure of human stratum corneum determined with small angle X-ray scattering, *J. Invest. Dermatol.*, 97 (1991) 1005–1012.
- [14] R.O. Potts, G.M. Golden, M.L. Francoeur, V.H.W. Mak and R.H. Guy, Mechanism and enhancement of solute transport across the stratum corneum, *J. Controlled Release*, 15 (1991) 249–260.
- [15] J.A. Bouwstra, G.S. Gooris, M.A. Salomons-de Vries, J.A. van der Spek and W. Bras, Structure of human stratum corneum as a function of temperature and hydration: a wide-angle diffraction study, *Int. J. Pharm.*, 84 (1992) 205–216.
- [16] J.B. Phipps and J.R. Gyory, Transdermal ion migration, *Adv. Drug Delivery Rev.*, 9 (1992) 137–176.
- [17] G.B. Kasting and J.C. Keister, Application of electrodiffusion theory for a homogeneous membrane to iontophoretic transport through skin, *J. Controlled Release*, 8 (1989) 195–210.
- [18] G.B. Kasting and L.A. Bowman, Electrical analysis of fresh human skin: a comparison with frozen skin, *Pharm. Res.*, 7–11 (1990) 1141–1145.
- [19] L.V. Chernomordik, S.I. Sukharev, I.G. Abidor and Y.A. Chizmadzhev, Breakdown of lipid membranes in an electrical field, *Biochim. Biophys. Acta*, 736 (1983) 203–213.
- [20] W.D. Stein, *Transport and Diffusion Across Cell Membranes*, Academic Press/Harcourt Brace Janovich, New York, 1986.
- [21] K.C. Madison, D.C. Swartzendruber, P.W. Wertz and D.T. Downing, Presence of intact intercellular lipid lamellae in the upper layers of the stratum corneum, *J. Invest. Dermatol.*, 88(6) (1987) 714–718.
- [22] M. Ponc, A. Weerheim, J. Kempenaar, A.-M. Mommaas and D.H. Nugteren, Lipid composition of cultured human keratinocytes in relation to their differentiation, *J. Lipid Res.*, 29 (1988) 949–962.
- [23] P.W. Wertz, D.C. Swartzendruber, D.J. Kitho and K.C. Madison, The role of corneocyte lipid envelopes in cohesion of stratum corneum, *J. Invest. Dermatol.*, 93 (1989) 169–172.